

Dynamic Modelling of a Hybrid Solar Thermal/electric Energy Storage System for Application in Residential Buildings

Andrea Frazzica¹, Valeria Palomba¹, Francesco Sergi¹, Marco Ferraro¹, Luisa F. Cabeza², Gabriel Zsembinszki², Eduard Oró², Sotirios Karellas³, Stratis Varvagiannis³, Johann Emhofer⁴, Tilman Barz⁴

¹ Istituto di Tecnologie Avanzate per l'Energia CNR-ITAE, Messina (Italy)

² GREiA Research Group, INSPIRES Research Centre, Universitat de Lleida, Lleida (Spain)

³ Lab. of Steam Boilers and Thermal Plants, National Technical University of Athens, Athens (Greece)

⁴ Austrian Institute of Technology AIT, Energy Department, Vienna (Austria)

Abstract

The present paper presents the dynamic modelling of a hybrid thermal/electric energy storage for residential applications. Two systems are considered, which are suitable for application in Continental and Mediterranean climates. Both systems are suitable for the provision of heating, cooling and domestic hot water, but the Continental system is optimized for heating and domestic hot water production, whereas the Mediterranean system is optimized for the covering of cooling demands. The models are realized in Dymola/Modelica environment and are structured according to a modular approach, using only self-developed components or open source libraries. An adsorption module, used for thermal energy storage purposes, a battery pack, used for electrical storage, latent heat storages and heat pumps are the main components modelled. The integration in sub-system and the typical operation during one day under reference conditions are shown, which prove the successful integration of several sub-modules.

Keywords: Modelica, hybrid storage, heating and cooling, modelling

1. Introduction

One of the critical aspects related to the increasing share of renewables at the building scale is the management of surplus of electricity produced (Schwarz et al., 2018). Indeed, the European Commission (European Commission, 2016) is strongly promoting the self-consumption in order to further support the integration of renewables in buildings. In such a context, different approaches for the optimization of the self-consumption in distributed energy systems were reported in the literature. One of the most common approaches, widely analysed and tested, is the integration of electric storage to support the generation from PV (Camilo et al., 2017; Lorenzi and Silva, 2016; Schram et al., 2018). However, this solution entirely relies on electricity generation. Different solutions proposed include the exploitation of weather forecasts to improve the system control strategy (Petrollese et al., 2018), the development of power-to-heat systems to convert excess of electricity into heat for space heating and cooling applications (Battaglia et al., 2017), and the pooling of different heat pumps together to increase the flexibility of electricity market and grid (Spreitzhofer et al., 2018). Concerning the latter solution, based on the efficient conversion of electricity into heat, the integration of advanced technologies for thermal and electric storage is mandatory, in order to achieve high storage density as well as to guarantee the necessary flexibility in operation (Bloess et al., 2018).

A general classification of the available technologies is given in Bloess et al., 2018, the primary distinction being between centralized and decentralized solutions. Since in many European areas the centralized systems are limited to heating solutions, or do not cover large areas, the development of efficient decentralized systems is mandatory. Among the solutions available, a vast number focuses on the integration of gas-fired and electric heat pumps/boilers (Heinen et al., 2016). However, the application of thermal energy storage is still limited, even though it is considered a promising solution (Yilmaz et al., 2018). Moreover, the solutions tested and investment analysis are often centred on Central and Northern European countries only (Yilmaz et al., 2018), where heating demand represents the main contribution to the building energy consumption.

In this context, the H2020 project HYBUILD proposes the use of two innovative compact hybrid electrical/thermal energy storage systems for stand-alone and district connected buildings. The two concepts will be specifically developed for ensuring comfort condition in residential buildings located in two different climates: one for

Mediterranean climate, where cooling season operation is particularly relevant, and another one for Continental climate, where the heating season operation is most important. Both systems will be able to efficiently cover also heating and cooling demand, respectively.

One of the main difficulties in the proper operation of the system is the integration of the core components and the development of a suitable management strategy. To this aim, it is mandatory to develop a reliable simulation tool, able to accurately describe the operation of the system. The present paper hence focuses on the dynamic simulation of the innovative hybrid thermal/electric storage solution proposed. The model was implemented in Dymola/Modelica environment using open source or self-developed components. A modular structure was followed, specifically focusing on an easy integration of the different components.

2. The HYBUILD concept

The proposed system will address two different concepts of hybrid energy storage: one mainly dedicated to the production of cooling energy, for Mediterranean countries (e.g. Spain, Italy, Greece, Cyprus, Portugal), and the other one, mainly dedicated to the delivering of heating energy, for the Continental countries (e.g. Austria, France, Germany, Switzerland, Denmark).

2.1 Mediterranean system

The proposed hybrid electric/thermal storage concept for Mediterranean climates aims at the integration of an electrically powered compression heat pump (HP) with a thermally driven sorption storage module and a battery pack. The HP will also be equipped with a latent heat thermal energy storage (LHTES) module. The proposed concept is reported in Figure 1a. The working principle is as follows: the electrical energy produced by the renewable source (PV panels) is directly connected, by means of a DC bus, to a DC powered vapour compression HP, which produces cooling energy for the building demand. On its evaporator side, a properly sized heat exchanger (HEX) and with a LHTES module is installed, in order to increase the storage capacity of the system, to stabilize the working boundary conditions of the compression HP, and to reduce the on/off period needed to follow the load evolution during the day. The condenser of the vapour compression chiller is coupled with the evaporator of the sorption storage, which produces DHW, exploiting solar thermal collectors as primary source to drive the desorption phase. In standard operation, the evaporator of the sorption storage module cools down the condenser of the compression HP, thus reducing its temperature lift between evaporator and condenser, resulting in enhanced efficiency in terms of electrical COP, that can even reach values above 6.0, which are about two times higher than the state-of-the-art HPs (Vasta et al., 2018). This will reflect in a reduced request of electrical energy to produce the cooling energy needed to cover the end-user's demand. Furthermore, solar thermal collectors and district heating network in case of district-connected buildings, also allow covering the DHW demand, and an electric storage allows increasing the operating flexibility of the system. Thanks to the reversibility of the operating mode of both compression HP and sorption storage, the system can also operate in heating mode, increasing the share of renewable, both thermal and electrical, to provide space heating in winter season.

2.2 Continental system

The hybrid storage concept for Continental climate is based on a HP, a LHTES for DHW production and an electrical storage. Contrary to the Mediterranean solution, the prioritized operation is heating during winter and the production of domestic hot water, whereas cooling during summer plays a minor role compared to the other two. The system proposed is shown in Figure 1b.

In this case, the heat sources are the air-source DC-powered HP and the PV panels for energy production. The operation is as follows: the electrical energy produced by the PV panels is used to drive the HP, which produces the heating energy for provision to the building. In the HP, a LHTES is integrated, is charged by the hot gas at the compressor outlet that can be used for DHW production. This storage can be charged slowly during the day, increasing the energy efficiency compared to direct DHW heating. Furthermore, an innovative sensible water storage with a high heat exchanger surface will be used inside the building to provide enough hot water within a short time. During summer, the air-source heat pump operates in reverse mode, for moderate cooling of the building.

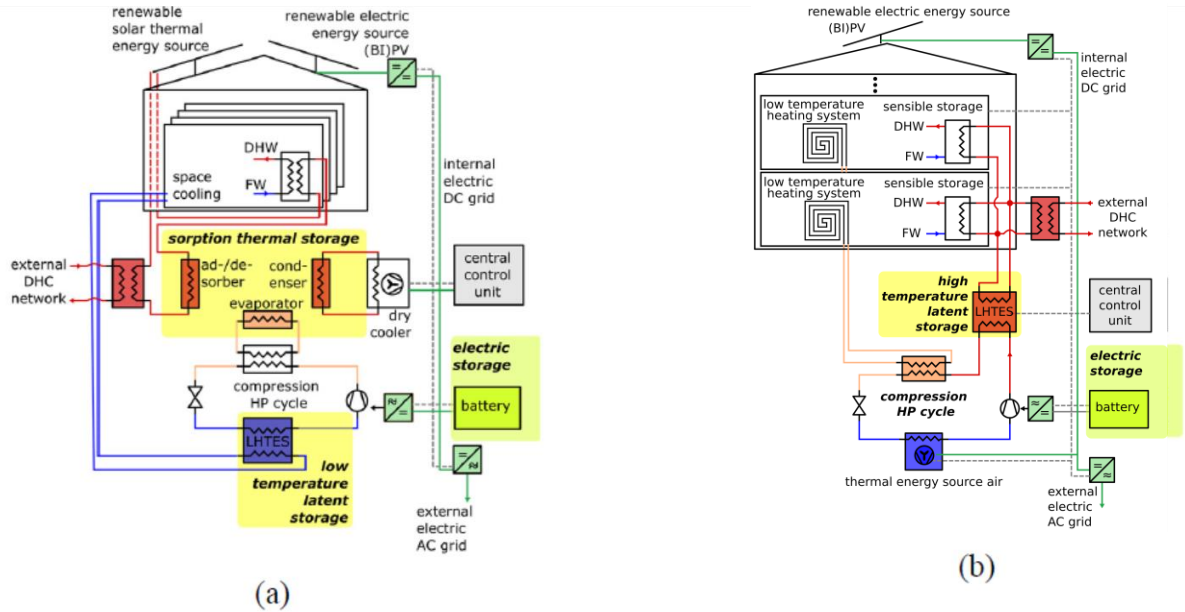


Figure 1. Schematic of the proposed system for hybrid thermal/electric storage, focusing on the provision of (a) cooling and (b) heating

3. Modelling approach

The target for the activity proposed is to describe both the Mediterranean and Continental hybrid sub-systems with models that are scalable, modular and easily integrated in different system configurations. The main features that the developed models possess are:

- utilization of open source libraries and components;
- easy connection to other components; and
- possibility to obtain useful results for the integration of the sub-system into the whole system.

The chosen modelling environment is Dymola, which represents a pre- and post-processing simulation platform for the open source language Modelica, which has already been proven to be suitable for the modelling of solar systems (Rodat et al., 2018). All the models were realised using self-developed components as well as components from Thermocycle (Quoilin et al., 2014) and CoolProp libraries (Bell et al., 2014).

4. Models of the core components

In the present section, important models for the core components of the sub-system will be described, whereas their integration into the whole sub-systems will be presented in the next section.

4.1 Adsorption module

The model structure is presented in Figure 2. It consists of four main components and an auxiliary valve that is used to continuously refill the refrigerant into the evaporator. The main components of the model are the adsorbers, the condenser and the evaporator, each of them consisting of two sub-components: an equilibrium model and a heat exchange model. The equilibrium model is the water/water vapour equilibrium for the condenser and the evaporator and the adsorption equilibrium model, defining the uptake as a function of pressure and temperature, in the adsorber. The approach followed is similar to that proposed for adsorption chillers by (Lanzerath et al., 2015; Schicktanz and Núñez, 2009), which proved to be reliable and suitable to describe, after a proper calibration, the operation of the systems considered. The model for the heat exchange on the heat transfer fluid (HTF) side is taken from Thermocycle library. It includes equations for mass, energy and momentum balance.

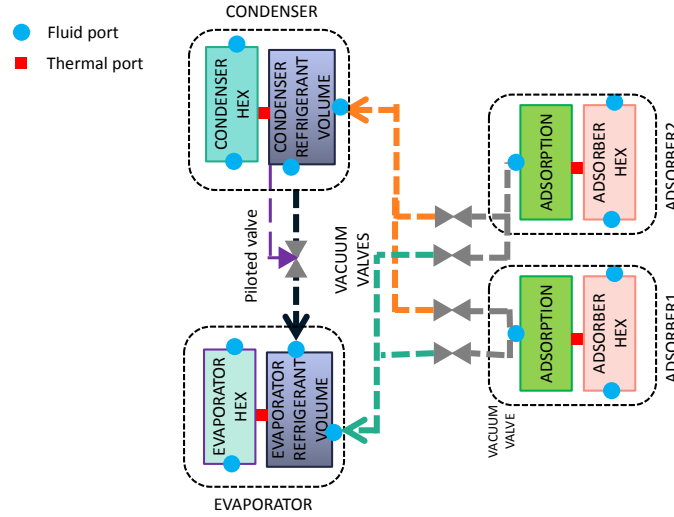


Figure 2. Layout of the model of the adsorption module

The model for the adsorption module results from the mass and energy conservation inside the adsorber. Energy conservation is expressed as:

$$\left(m_{sorb}c_{p_{sorb}} + w \cdot m_{sorb}c_{p_{ref}}\right) \frac{dT_{sorb}}{dt} = \dot{Q}_{ads} + \dot{m}_{ref}h_{ads} - m_{sorb}c_{p_{sorb}}T_{sorb} \frac{dw}{dt} \quad (1)$$

The terms on the left-hand side represent the sensible heat stored in the adsorbent, whereas the terms on the right-hand side represent the heat transferred through conduction and the mass exchange. For simplicity's sake, the heat of adsorption h_{ads} was considered constant.

The equilibrium conditions for temperature T_{sorb} , pressure p_{ads} and uptake w (the amount of refrigerant adsorbed onto the material) can be described by means of different equations according to the adsorbent chosen. For zeolite and zeotype materials, one common approach is to use Dubinin-Ashtakov (DA) correlation (Frazzica and Freni, 2017):

$$w = w_0 \exp \left[- \left(\frac{A}{E} \right)^n \right] \quad (2)$$

where w_0 [g/g] and n [-] are empirical constants, and A [kJ/mol] is the adsorption potential:

$$A = -RT_{sorb} \log \frac{p_{ads}}{p_{sat}} \quad (3)$$

The flow rate of refrigerant adsorbed is a function of the uptake variation in time:

$$\dot{m}_{ref} = m_{sorb} \frac{dw}{dt} \quad (4)$$

Adsorption kinetics is described by means of a Linear Driving Force (LDF) approach (El-Sharkawy, 2011):

$$\frac{dw}{dt} = \beta(w_{eq} - w) \quad (5)$$

where the constant β [t^{-1}] is calculated as (Lanzerath et al., 2015):

$$\beta = \frac{15}{r_{sorb}^2} D \quad (6)$$

where D [$m^2 s^{-1}$] is a diffusion coefficient. Saturation properties of the refrigerant are calculated using CoolProp library.

The condenser and the evaporator of the adsorption module consist of a vacuum vessel with a heat exchanger partially immersed into the liquid refrigerant. Water/water vapour equilibrium is described by mass and energy balance equations:

$$\frac{dm}{dt} = \dot{m}_v + \dot{m}_l \quad (7)$$

In the case of the condenser, the incoming fluid is vapour at the temperature of the adsorber and the outlet fluid is

$$\frac{dU}{dt} = \dot{H}_v + \dot{H}_l + \dot{Q} \quad (8)$$

liquid having saturation enthalpy. Conversely, in the case of the evaporator, the incoming fluid is liquid at the temperature of the condenser and the outlet fluid is vapour having saturation enthalpy. The term \dot{Q} [W] represents the heat flow between the saturated refrigerant and the surface of the heat exchanger.

4.2 Compression heat pump for the Mediterranean system

The model of the heat pump is based on the acausal modelling technique and is mainly composed of four elements: the compressor, the heat exchangers for the evaporator and condenser, and the expansion valve.

The modelling approach followed for the heat exchangers is the Moving Boundaries technique. Moving boundaries models are generally faster compared to finite volume implementations, without loss in model's accuracy (Bendapudi et al., 2008). The moving boundary implementation used follows the equations described by Willatzen (Willatzen and Pettit, 1998). However, as an enhancement to the original equations proposed by Willatzen and similarly to the standard moving boundary implementation in ThermoCycle, the heat transfer between the primary and the secondary fluid is calculated by means of ϵ -NTU method, instead of calculating it using the temperature difference between the corresponding cells. A schematic representation of the model and heat contributions in each zone are shown in Figure 3 for the case of the condenser. The model for the evaporator is similar to that for the condenser, with the difference of having two zones instead of three (since the refrigerant enters the evaporator in two phase state).

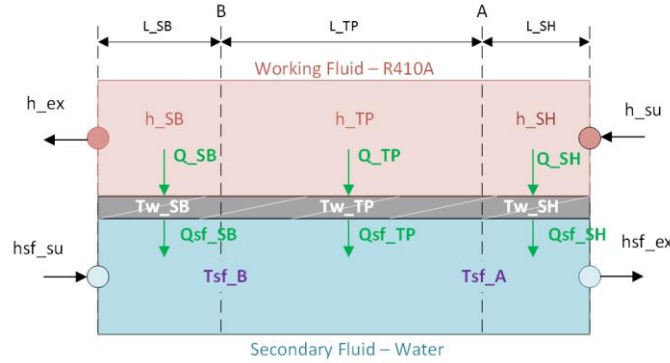


Figure 3. Schematic representation of the moving boundaries formulation in the condenser of the heat pump for the Mediterranean system

The model for the compressor is a steady state model, based on the volumetric and isentropic efficiency. This model is derived from the standard compressor model included in ThermoCycle library, while the volumetric and isentropic efficiencies are calculated as functions of the pressure ratio r_p (Byrne et al., 2012):

$$e_{vol} = 1 - C \left(r_p^{\frac{1}{n}} - 1 \right) \quad (9)$$

$$e_{is} = K(1 - e^{-b \cdot r_p}) \quad (10)$$

In both equations, C, n, K and b are constants which must be calibrated to manufacturer efficiency curves.

The mass flow rate transferred by the compressor is calculated using the following equation:

$$\dot{m}_f = e_{vol} \frac{N_{rot}(RPM) \cdot V_s \cdot \rho_{SU}}{60} \quad (11)$$

where V_s the swept volume of the compressor, which is the only parameter of the model and was given by the manufacturer as $V_s = 102 \cdot 10^{-6} m^3$. The enthalpy at the outlet of the compressor using the definition of the isentropic efficiency:

$$h_{ex} = h_{su} + \frac{(h_{ex,is} - h_{su})}{e_{is}} \quad (12)$$

The shaft power needed for the compression is calculated as:

$$P_{shaft} = \dot{m}_f (h_{ex} - h_{su}) \quad (13)$$

The thermostatic expansion valve model is based on the standard valve component of the ThermoCycle library,

controlled by a PID controller which maintains the superheating at a desired value. While this implementation is actually an Electronic Expansion Valve (EEV) its operation is similar to the standard TEXV's operation. The expansion is assumed to be isenthalpic.

The mass flow rate through the valve is calculated from the pressure drop using the following expression:

$$\dot{m}_f = A \cdot \sqrt{2 \cdot \rho_{SU} \cdot \Delta p} \quad (14)$$

where A is the area of the orifice inside the valve, which changes linearly with the control signal.

The superheating of the fluid exiting the evaporator is calculated in real time by measuring its pressure and temperature. The degree of opening of the valve is controlled using a PID algorithm in order to achieve the desired superheating. The overall layout of the heat pump in Dymola environment is shown in Figure 4.

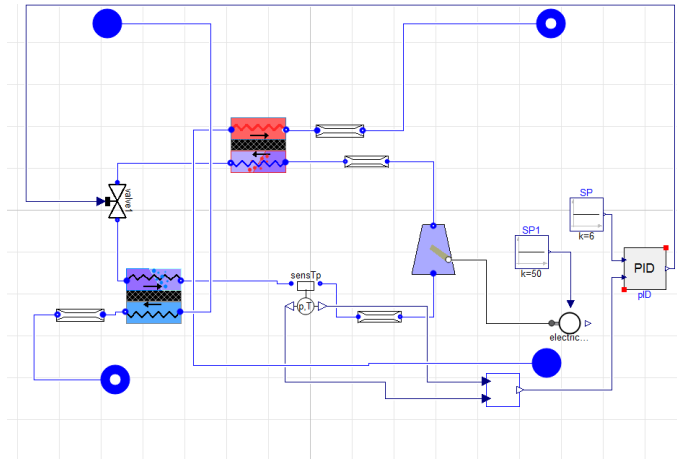


Figure 4. Schematics of the heat pump model in the Dymola environment

4.3 Latent heat thermal energy storage module

The LHTES module consists of a 3-fluid (refrigerant, PCM, and water) heat exchanger (RPW-HEX). The RPW-HEX is a rectangular container. The internal design consists of a parallel arrangement of rectangular passages for water and refrigerant with rectangular layers of PCM in between. Fluid passages and PCM layers are arranged sequentially. In order to study the thermal behaviour of the RPW-HEX, a 2D numerical model was developed. Because of symmetry of the RPW-HEX design, the relatively abundance of passages and layers, and the thermal insulation of the storage container it is assumed that all parallel passages and PCM layers behave identically. Therefore, only the relevant section of the entire component was considered in the model, which considers solely one refrigerant + water + PCM layer, as schematically shown in Figure 5.

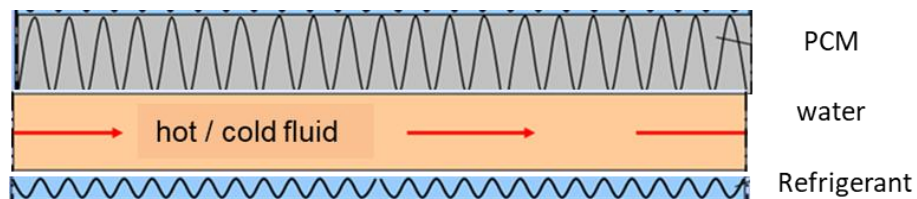


Figure 5. Schematics of the control volume assumed for the RPW-HEX simulation

The discretization of each of the control volume is shown in Figure 6. Notice that there are three possible working conditions, depending on whether only one or both the refrigerant and water flows are moving within the RPW-HEX:

- Refrigerant is charging the PCM (Figure 6-left). There is no water circulation.
- Water is discharging the PCM (Figure 6-center). There is no refrigerant circulation.
- Refrigerant is transferring heat/cold to the water (Figure 6-right). In this situation the PCM will be partially charged.

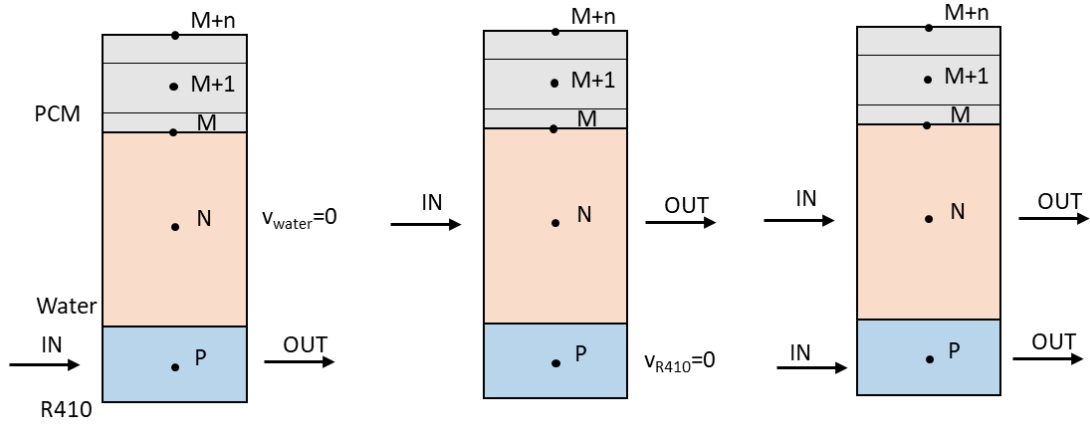


Figure 6. Schematics of the discretization of the control volume assumed for three different scenarios: left: PCM charging, centre: PCM discharging, right: standard working conditions

The two-dimensional heat transfer during charging/discharging is governed by the following equation:

$$\sum \dot{Q} + (\dot{m}_{in} \cdot h_{in}) - (\dot{m}_{out} \cdot h_{out}) = \rho \cdot c_p \cdot \frac{\Delta T}{\Delta t} \cdot dV \quad (15)$$

In the model, the number of nodes taken in the flow direction was 100, while in the vertical direction solely one node is used for the refrigerant and water, respectively, while 5 nodes were considered for PCM. The system of algebraic linear equations extracted from the finite volume method was solved using Gauss Seidel iterative method with a time step of 1 second. The solution was found to be mesh-independent based on the above nodes selection.

An important parameter of the RPW-HEX is its state of charge (SoC), which is used to indicate the extent to which a LHTES module is charged relative to storable latent heat (see definition of SoC (Barz et al., 2018)). The SoC, denoted by Ξ , is calculated as the geometric mean of local (liquid mass) phase fraction fields $\xi(x,y,z)$, where x, y, z represent spatial coordinates of the PCM contained in the LHTES module. The phase fraction fields $\xi(x, y, z)$ can be directly derived from the temperature fields $T(x, y, z)$.

As stated above, a two dimensional geometry was considered, with a coordinate pointing in the water or refrigerant flow direction (x on the domain $0 \leq x \leq L$), and one coordinate pointing into the PCM layer perpendicular to the first coordinate (y on the domain $0 \leq y \leq d$). For this two dimensional planar geometry of the PCM, the state of charge Ξ is calculated as geometric mean as:

$$\Xi = \frac{\int_0^L \int_0^d \xi(x, y) dy dx}{L \cdot d} \quad (16)$$

The integration of Eq. (16) needs to be carried out numerically.

For the Continental sub-system the RPW-HEX is used as hot storage, while for the Mediterranean sub-system it is used as cold storage. Accordingly, different SoC are defined to account for the fact that the hot storage is fully charged if all PCM is in the liquid state, while the cold storage is fully charged when the PCM is in solid state:

$$\begin{aligned} \Xi^{\text{hot}} &:= \Xi \\ \Xi^{\text{cold}} &:= 1 - \Xi \end{aligned} \quad (17)$$

The numerical RPW-HEX model was implemented in Modelica/Dymola simulation software in order to facilitate sub-system simulations, and to develop and evaluate its design and basic control settings under different operating scenarios. A minimal test example (no connection to other sub-system components) for the Mediterranean sub-system is shown in Figure 7.

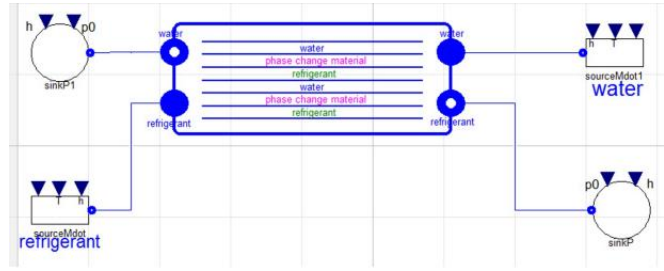


Figure 7. Dymola RPW-HEX model object of the MED system. This minimal test example uses fixed water and refrigerant inlet conditions

The implementation is based on the state-of-the-art ThermoCycle library model components (Quoilin et al., 2014). These model components are used to represent the water and refrigerant flow through the RPW-HEX internal parallel passages. Corresponding components are modifications of ThermoCycles so called “Flow1D” and “Cell1D” fluid flow components, see

Figure 12. Modifications concern the addition of a second heat port to account for: heat transfer between water (or refrigerant) passage and PCM, and heat transfer between water and refrigerant passage. The use of ThermoCycle standard fluid flow components, enables the user to select between different (available) options for state-of-the-art numerical discretization schemes and options for well-established heat transfer correlations.

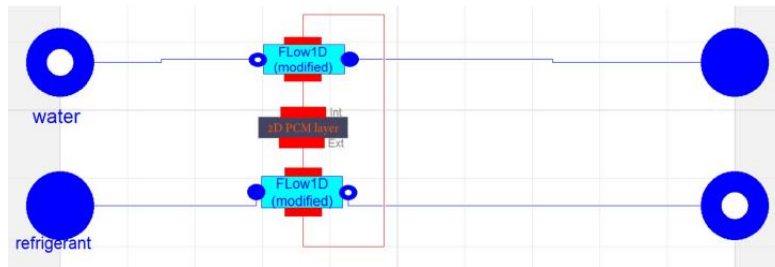


Figure 8. Graphical representation of model classes used to define the Dymola RPW-HEX model of the Mediterranean sub-system. Heat ports and connectors between the balance envelopes of the water passage, refrigerant passage and the PCM layer are shown in red.

The PCM layer is modelled using an ThermoCycle adapted heat flow component, namely a wall element. This component can be directly connected to the fluid flow elements using ThermoCycle thermal ports. According to the three-fluid RPW-HEX model, a two-dimensional PCM model is implemented and apparent (effective) PCM properties are used. The user can select between different phase transition models, and the SoC is calculated as described above.

4.4 Electrical storage model

The model used for the electrical storage is based on Sheperd model, that describes the electrochemical behaviour of a battery in terms of voltage and current by excluding thermal and quantum phenomena (Hanlei Zhang and Mo-Yuen Chow, 2010; Shepherd, 1965). The model was improved by introducing the Peukert equation that quantifies the capacity reduction according to output current from the battery (Leksono et al., 2013). The reference equations of the model are the following:

$$V = E_0 - J \frac{C_{max}}{C_{max} - C(t)} i + H \exp[-P \cdot C(t)] - R_0 i \quad (18)$$

$$V = E - R_0 i$$

where: V is the cell voltage [V], E₀ the Open Circuit Voltage (OCV) [V], J the polarization factor [Ah⁻¹], C_{max} the maximum capacity of the battery [Ah], C(t) the charged/discharged capacity at time t, i the cell current [A], H the exponential voltage component [V], P the exponential capacity component [Ah⁻¹], R₀ the internal resistance [Ω].

The SOC is estimated as:

$$SOC = \int \frac{i}{C_{max}} dt \quad (19)$$

5. Models of the sub-systems

5.1 Mediterranean sub-system

The Mediterranean hybrid sub-system comprises four main components: the sorption module, the compression heat pump, which includes the RPW-HEX module, and the electrical storage. Figure 9a shows Dymola diagram of the complete sub-system, including the sources and sinks that simulate the other components in the overall system and the electric parameters from the PV panels. The integration of the heat pump with the RPW-HEX is shown in detail in Figure 9b. What is clear is that the approach followed proved to be effective, since it was easily possible to connect all the components and realise a complete model of the sub-system.

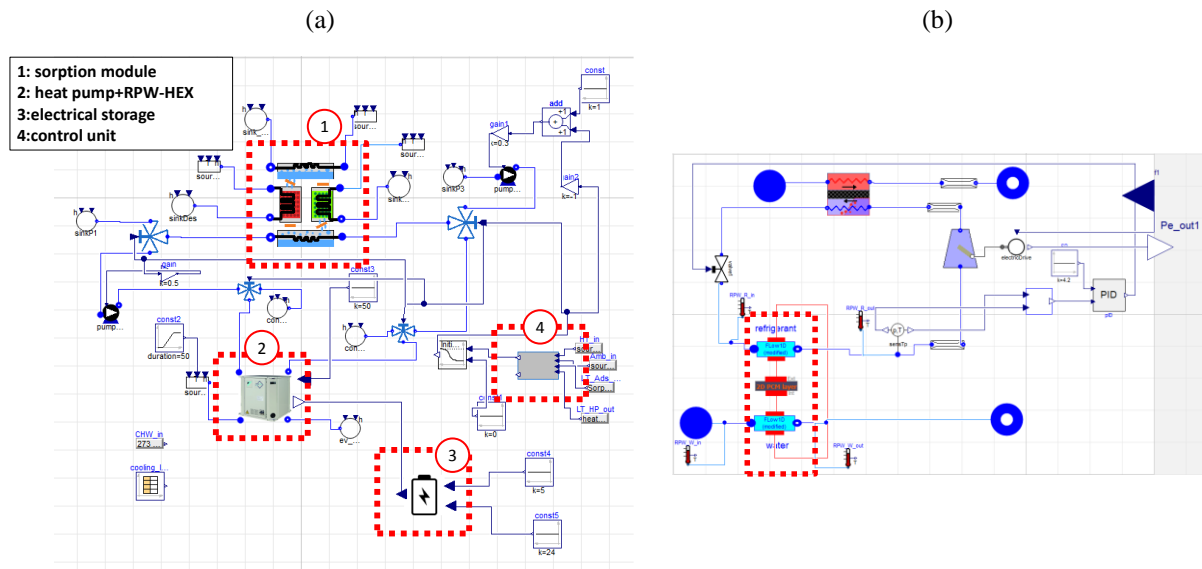


Figure 9. (a) Dymola diagram of the Mediterranean sub-system; (b) detail of the integration of the heat pump with the RPW-HEX.

5.2 Continental sub-system

The Continental hybrid sub-system consists of mainly three different types of storages: the latent storage (RPW-HEX) integrated in the compression heat pump cycle, the decentralized sensible DHW storages, and the electric storage (see Figure 1b and Figure 10). In the simulations (Figure 10) an option was investigated, where the process water to the decentralized DHW storage flows first through the condenser and afterwards through the latent storage. Furthermore, a simple building model working as a heat sink for the heating system, which considers a constant heat transfer coefficient, a representative mass of the building, and the ambient temperature was used.

During heating operation, solely the heat from the condenser is extracted with the aid of the process water flowing through the secondary side whereas in the case of DHW generation the process water flows also through the RPW-HEX after leaving the condenser. With the aid of two three-way valves and three ramp-modules, operation can be switched between heating and DHW generation.

6. Results

6.1 Mediterranean sub-system

In order to test the model of the sub-system, operation on a typical day was considered. In particular, weather data for Aglantzia (CY), one of the locations chosen in the project for pilot installation were used, as well as the cooling demand for the building where the installation will take place. A reference day in August (20th) was chosen. For simplicity sake a constant heat source temperature of 90°C was considered, taking into account that the heat coming from Fresnel collectors in the installation for HYBUILD will be collected in a sensible storage.

Results from 9 am to 3 pm are shown in Figure 11. In particular, Figure 11a shows the temperatures in the circuits of the adsorption module and the heat pump. It is possible to notice that the cyclic operation of the adsorption module induces periodic rising in the temperature of the condenser of the heat pump, but the average inlet to the condenser of the heat pump is below 20°C, thus reducing more than 10°C the temperature lift of the unit. Figure 11b shows the powers in the different components of the adsorption module and the heat pump, calculated from the thermodynamic states of the fluids in each component. It is possible to notice that the power in the condenser of the heat pump corresponds to the average power from the evaporator of the adsorption module. Moreover, at each phase change

there is a peak in the power absorbed/released from the adsorbers, due to the sensible heat and sorption heat of the material.

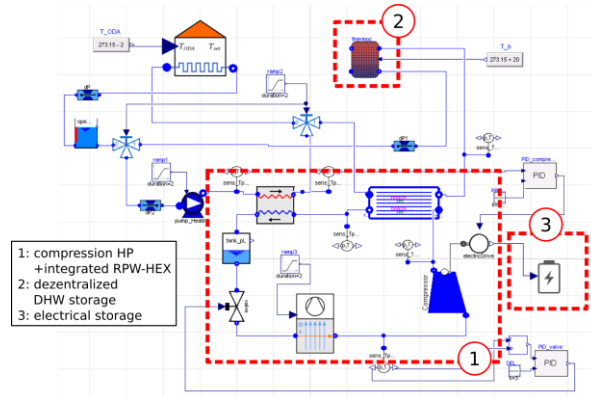


Figure 10. Dymola diagram of the Continental sub-system

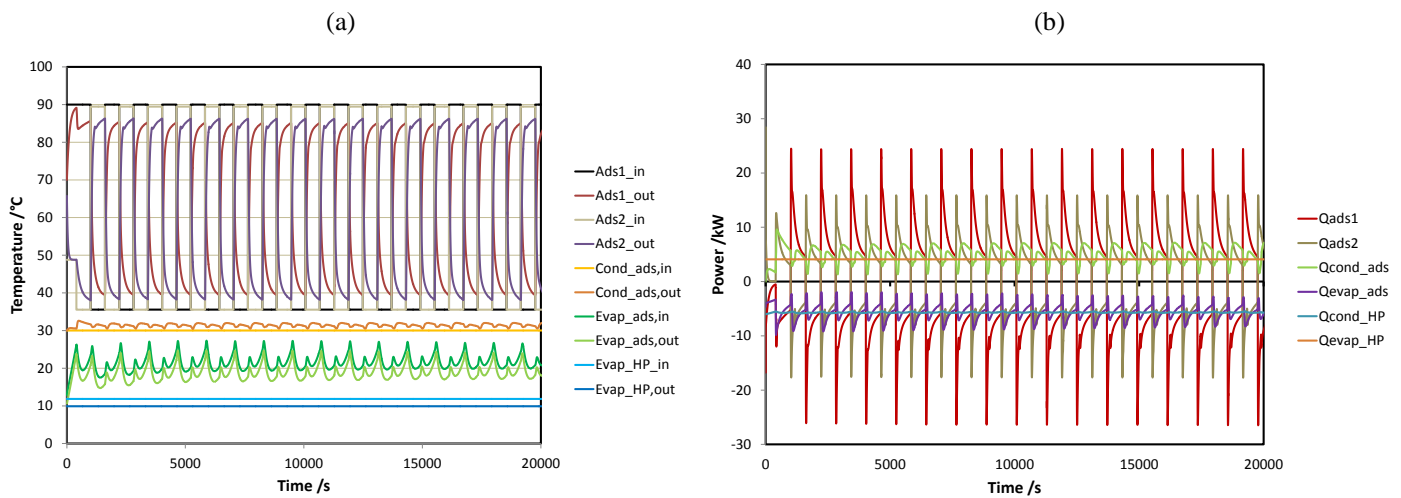


Figure 11. Temperatures (a) and thermal powers (b) in the circuits of the sorption module and heat pump for the reference conditions

6.2 Continental sub-system

In the following, the Continental sub-system will be discussed for a typical ambient condition in winter. The outdoor temperature was 2 °C in this scenario. The building itself is already heated to its steady-state temperature of 20.4 °C at $t=0$ s. The DHW storage needs to be charged and had an initial temperature of 15 °C at the bottom of the water tank and 35°C at the top (see

Figure 12a). The RPW-HEX is filled with a PCM that has a switching temperature at around 64 °C. At $t=0$ s the RPW-HEX has a uniform temperature of 62 °C, hence nearly no latent energy is stored at the beginning of the simulation (SoC = 1.2 %).

After starting the heat pump at $t=0$ s in heating mode (no mass flow to decentralized DHW storage), the system was switched after 4000 s to DHW generation mode. For a fair comparison we will observe solely the behaviour of the system after stabilization of the heat pump between SoCs of 5 % or in other words between $t=426$ s and $t=4714$ s in our example. Hence, the building heating time will last for around 1 hour before the heat pump switches for 12 minutes into DHW generation mode. During heating operation, the RPW-HEX will be charged up to a maximum of 35 % before the hydraulic valves are switched to DHW generation and slow down the process water. During DHW generation, the RPW-HEX will be discharged down to 5 % again. Contrary to conventional systems, the condensing pressure/temperature controlled via the temperature of the process water outlet and the compressor rotational speed should stay nearly the same during heating and DHW generation operation. The extra thermal energy to heat up the process water to DHW-temperatures ($>60^{\circ}\text{C}$) will solely be extracted from the RPW-HEX in DHW generation mode. In Figure 12b (green, dashed line), one can see that the implemented PID-controller does not manage to limit the outlet condenser temperature $\vartheta_{wa,con}^{(out)}$ perfectly during DHW generation. This is actually a difficult task as the compressor speed (and therefore the power consumption) decreases and the inlet temperature to the secondary side

of the condenser $\vartheta_{wa,con}^{(in)}$ (blue solid line in Figure 12b) varies over the time. One can see clearly, that the stored energy in the RPW-HEX is sufficient to provide process water with a charging temperature of about 63°C (red dotted line in Figure 12b) for about 12 minutes which heats the top layer or the decentralized storage to about 50°C.

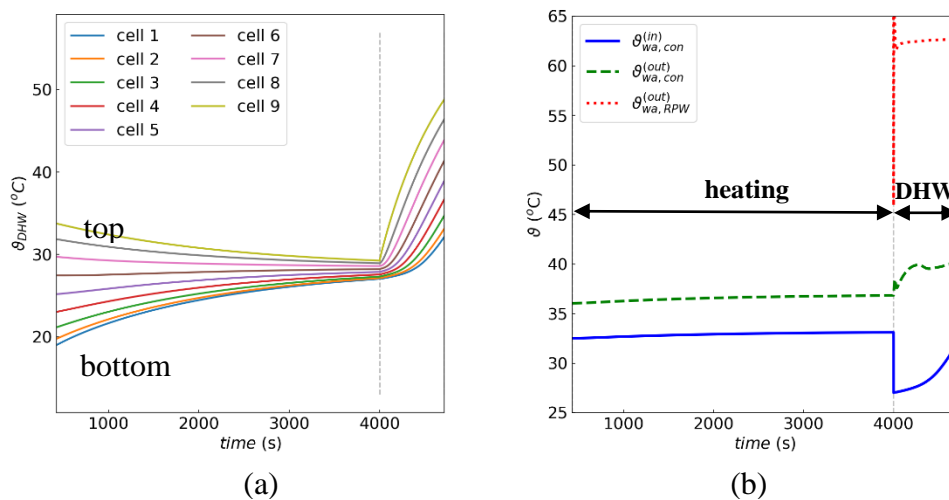


Figure 12. (a) Vertical temperature distribution in the decentralized DHW-storage from the top (cell 9) to the bottom (cell 1) and (b) temperatures on the process water side of the condenser and the RPW-HEX

7. Conclusions and on-going activities

The development of the models for two hybrid thermal/electrical storage systems for Continental and Mediterranean climates were presented. The models were realized in Dymola/Modelica environment, using a modular approach: the core components were modelled using open source libraries and self-developed components. Integration of the components and verification of the operation of the sub-systems under reference operating conditions were carried out. Current activities are aimed at the realization of prototypes of the core components and their laboratory testing, in order to validate and calibrate the realized models. The developed models will be subsequently used to test the management strategies and for techno-economic analysis.

8. Acknowledgments

This project has received funding from the European Union's Horizon 2020 research and innovation programme under grant agreement No 768824 (HYBUILD).

9. References

- Barz, T., Seliger, D., Marx, K., Sommer, A., Walter, S.F., Bock, H.G., Korkel, S., 2018. State and state of charge estimation for a latent heat storage. *Control Eng. Pract.* 72, 151–166. doi:10.1016/J.CONENGPRAC.2017.11.006
- Battaglia, M., Haberl, R., Bamberger, E., Haller, M., 2017. Increased self-consumption and grid flexibility of PV and heat pump systems with thermal and electrical storage. *Energy Procedia* 135, 358–366. doi:10.1016/J.EGYPRO.2017.09.527
- Bell, I.H., Wronski, J., Quoilin, S., Lemort, V., 2014. Pure and Pseudo-pure Fluid Thermophysical Property Evaluation and the Open-Source Thermophysical Property Library CoolProp. *Ind. Eng. Chem. Res.* 53, 2498–2508. doi:10.1021/ie4033999
- Bendapudi, S., Braun, J.E., Groll, E.A., 2008. A comparison of moving-boundary and finite-volume formulations for transients in centrifugal chillers Comparaison entre les formulations aux limites mobiles et ´ gimes transitoires des aux volumes finis pour les re refroidisseurs centrifuges. *Int. J. Refrig.* 31, 1437–1452. doi:10.1016/j.ijrefrig.2008.03.006
- Bloess, A., Schill, W.-P., Zerrahn, A., 2018. Power-to-heat for renewable energy integration: A review of technologies, modeling approaches, and flexibility potentials. *Appl. Energy* 212, 1611–1626. doi:10.1016/J.APENERGY.2017.12.073
- Byrne, P., Miriel, J., Lénat, Y., 2012. Modelling and simulation of a heat pump for simultaneous heating and cooling. *Build. Simul.* 5, 219–232. doi:10.1007/s12273-012-0089-0
- Camilo, F.M., Castro, R., Almeida, M.E., Pires, V.F., 2017. Economic assessment of residential PV systems with

- self-consumption and storage in Portugal. *Sol. Energy* 150, 353–362. doi:10.1016/J.SOLENER.2017.04.062
- El-Sharkawy, I.I., 2011. On the linear driving force approximation for adsorption cooling applications. *Int. J. Refrig.* 34, 667–673. doi:10.1016/J.IJREFRIG.2010.12.006
- European Commission, 2016. European Commission, 2016. Communication from the Commission to the European Parliament, the Council, the European Economic and Social Committee and the Committee of the Regions and the European Investment Bank, Brussels.
- Frazzica, A., Freni, A., 2017. Adsorbent working pairs for solar thermal energy storage in buildings. *Renew. Energy* 110, 87–94. doi:10.1016/j.renene.2016.09.047
- Hanlei Zhang, Mo-Yuen Chow, 2010. Comprehensive dynamic battery modeling for PHEV applications, in: *IEEE PES General Meeting*. IEEE, pp. 1–6. doi:10.1109/PES.2010.5590108
- Heinen, S., Burke, D., O'Malley, M., 2016. Electricity, gas, heat integration via residential hybrid heating technologies – An investment model assessment. *Energy* 109, 906–919. doi:10.1016/J.ENERGY.2016.04.126
- Lanzerath, F., Bau, U., Seiler, J., Bardow, A., Bardow, E., 2015. Optimal design of adsorption chillers based on a validated dynamic object-oriented model. *Sci. Technol. Built Environ.* 21, 248–257. doi:10.1080/10789669.2014.990337
- Leksono, E., Haq, I.N., Iqbal, M., Soelami, F.X.N., Merthayasa, I.G.N., 2013. State of charge (SoC) estimation on LiFePO₄ battery module using Coulomb counting methods with modified Peukert, in: *2013 Joint International Conference on Rural Information & Communication Technology and Electric-Vehicle Technology (RICT & ICeV-T)*. IEEE, pp. 1–4. doi:10.1109/rICT-ICeVT.2013.6741545
- Lorenzi, G., Silva, C.A.S., 2016. Comparing demand response and battery storage to optimize self-consumption in PV systems. *Appl. Energy* 180, 524–535. doi:10.1016/J.APENERGY.2016.07.103
- Petrollese, M., Cau, G., Cocco, D., 2018. Use of weather forecast for increasing the self-consumption rate of home solar systems: An Italian case study. *Appl. Energy* 212, 746–758. doi:10.1016/J.APENERGY.2017.12.075
- Quoilin, S., Desideri, A., Wronski, J., Bell, I., Lemort, V., 2014. ThermoCycle: A Modelica library for the simulation of thermodynamic systems, in: *Proceedings of the 10th International Modelica Conference*. Lund, Sweden. doi:10.3384/ECP14096683
- Rodat, S., Baviere, R., Bruch, A., Camus, A., 2018. Dynamic simulation of a Fresnel solar power plant prototype with thermocline thermal energy storage. *Appl. Therm. Eng.* doi:10.1016/J.APPLTHERMALENG.2018.02.083
- Schick Tanz, M., Núñez, T., 2009. Modelling of an adsorption chiller for dynamic system simulation. *Int. J. Refrig.* 32, 588–595. doi:10.1016/J.IJREFRIG.2009.02.011
- Schram, W.L., Lampropoulos, I., van Sark, W.G.J.H.M., 2018. Photovoltaic systems coupled with batteries that are optimally sized for household self-consumption: Assessment of peak shaving potential. *Appl. Energy* 223, 69–81. doi:10.1016/J.APENERGY.2018.04.023
- Schwarz, H., Schermeyer, H., Bertsch, V., Fichtner, W., 2018. Self-consumption through power-to-heat and storage for enhanced PV integration in decentralised energy systems. *Sol. Energy* 163, 150–161. doi:10.1016/J.SOLENER.2018.01.076
- Shepherd, C.M., 1965. Design of Primary and Secondary Cells. *J. Electrochem. Soc.* 112, 657. doi:10.1149/1.2423659
- Spreitzhofer, J., Esterl, T., Schwalbe, R., Stifter, M., 2018. Pooling of smart heat pumps provides flexibility to the electricity market and grids. *IEA HPT Mag.*
- Vasta, S., Palomba, V., La Rosa, D., Mittelbach, W., 2018. Adsorption-compression cascade cycles: An experimental study. *Energy Convers. Manag.* 156, 365–375. doi:10.1016/j.enconman.2017.11.061
- Willatzen, M., Pettit, N.B.O.L., 1998. A general dynamic simulation model for evaporators and condensers in refrigeration. Part I: moving-boundary formulation of two-phase flows with heat exchange. *Int. J. Refrig.* 21, 398–403. doi:10.1016/J.IJREFRIG.1998.05.003
- Yilmaz, H.Ü., Keles, D., Chiodi, A., Hartel, R., Mikulić, M., 2018. Analysis of the power-to-heat potential in the European energy system. *Energy Strateg. Rev.* 20, 6–19. doi:10.1016/J.ESR.2017.12.009